

## Bifunctional Patterning of Mixed Monolayer Surfaces Using Scanning Probe Lithography for Multiplexed Directed Assembly

David A. Unruh, Clayton Mauldin, Stefan J. Pastine, Marco Rolandi, and Jean M. J. Fréchet\*

College of Chemistry, University of California, Berkeley, California 94720

Received February 24, 2010; E-mail: frechet@berkeley.edu

The development of methods for the production of substrates with different spatially resolved functionalities is highly desirable, as their impact may range from semiconductor fabrication to biology.<sup>1,2</sup> Surface-bound functionalities can serve as templates for the directed assembly of molecules or nano-objects, allowing the bottom-up fabrication of sensors, arrays, and devices. Several multicomponent patterning strategies have been reported, including orthogonal solvent treatments, plasma treatments, photolithography, and capillary force lithography.<sup>3</sup> An issue with some of these techniques is that they may not extend to the sub-100 nm feature size regime or may require harsh treatments or complicated syntheses. The use of scanning probe lithography (SPL) for nanoscale patterning is attractive because it allows high-resolution direct-write patterning,<sup>4</sup> real-time imaging of patterns, serial on-chip patterning of multiple functionalities, and mild processing conditions. We have previously reported an SPL technique for the local deprotection of surface-bound amines that utilizes the electric field produced by a positively biased sample and a grounded atomic force microscope (AFM) tip.<sup>5</sup> The ability to pattern a second functionality chemically distinct from amines in the same AFM patterning step would allow the assembly of complementary combinations of molecules with sub-100 nm features. Herein we report an electrochemically based SPL method where, depending upon the surface bias applied (Figure 1a), a redox-sensitive surface-bound molecule can be electrochemically reduced to yield an amine or the surface can be locally oxidized to produce an oxygen-rich species.

It has been established that the nanoscale water meniscus that forms between the surface and the tip of the scanning probe can mediate the controlled transfer of molecules from tip to surface,<sup>6</sup> the localized oxidation of both inorganic and organic surfaces,<sup>7</sup> and the electrochemical reduction of metals.<sup>8</sup> In comparison with oxidative methods, reductive SPL methods have not been as extensively investigated. We envisioned that through careful monolayer design we could use this water meniscus as a “nanoscale electrochemical cell” capable of performing local surface oxidation or reduction, depending upon the patterning conditions. To this end, we designed a triethoxysilane derivative (**1**) featuring a redox-active<sup>9</sup> trimethylbenzoquinone moiety. Amine patterns could thus be generated in monolayers based on **1** via the local reduction and subsequent lactonization of the departing benzoquinone moiety under the stimulus provided by the tip.

Figure 1b summarizes the reductively active surfaces used and their preparation. Benzoquinone-modified surface **2** had a typical thickness of  $0.63 \pm 0.27$  nm, as measured by ellipsometry, and a contact angle of  $70 \pm 4^\circ$ . In line with the reduction of other trimethylbenzoquinone-based surfaces,<sup>9b</sup> irreversible blanket reduction of **2** was demonstrated using cyclic voltammetry [CV; see the Supporting Information (SI)]. Support for this blanket modification was provided by surface contact angle measurements both before and after CV reduction. The contact angle after reduction ( $55^\circ$ ) approached that of an amine-terminated monolayer ( $51^\circ$ ). The

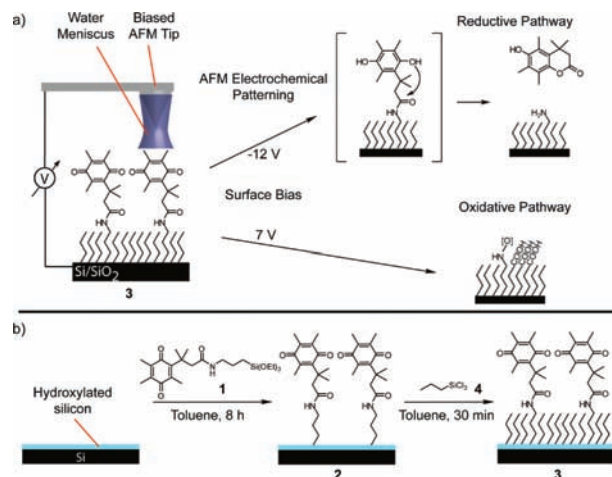


**Figure 1.** (a) Schematic of orthogonal AFM patterning on the benzoquinone/propyltrichlorosilane mixed monolayer **3**. (b) Syntheses of benzoquinone-modified surface **2** and mixed monolayer **3**.

surface coverage of **1** on surface **2** calculated from the CV data amounted to only  $\sim 18\%$  of the available Si(100) surface binding sites, likely as a result of steric interactions between the bulky quinoid groups of **1**.

Having confirmed macroscopic reduction, we next investigated SPL on **2**. Patterning experiments were performed in contact mode with doped silicon tips in an environment with  $70 \pm 5\%$  relative humidity. The grounded tip was translated at  $1\text{--}4 \mu\text{m/s}$  across the surface with a  $-12$  V bias applied to the surface, and lateral force microscopy was used to verify the surface modification. The darkened vertical lines in Figure 2a have a width of  $80 \pm 4$  nm and correspond to the modified areas. The vertical deflection of the tip did not change during patterning, and the corresponding postpatterned topography images do not show significant height changes; therefore, it is unlikely that the observed lines are due to scratching of the substrate. The difference in reduction bias between SPL and CV may be due to the lack of a supporting electrolyte in the water meniscus during SPL. The width of the patterned lines was found to depend upon the relative humidity, applied surface bias, and patterning speed (see the SI). Microscale patterning was also achievable using electrically conductive copper grids,<sup>10</sup> and

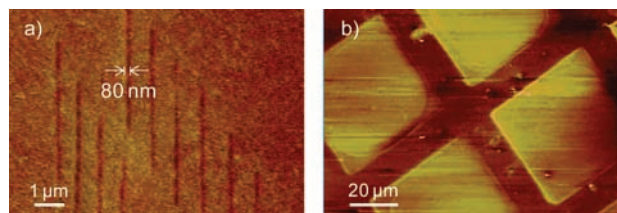


**Figure 2.** Lateral force microscopy images of (a) SPL-patterned and (b) copper-grid-patterned surfaces.

the lateral force microscopy image in Figure 2b clearly shows pattern transfer from the grid to the substrate. No evidence of patterning was observed under dry conditions (relative humidity <5%), which suggests that an electrochemical process is responsible for patterning, in contrast to other high electric field-based SPLs on organic monolayers.<sup>5,11</sup>

These patterned areas can act as templates for the directed assembly of various nano-objects through both ionic and covalent chemistries. For example, incubation of surfaces patterned either by SPL or on the microscale in a solution of C<sub>60</sub> provided raised regions ~0.8 nm in height, which is close to the expected diameter of an amine-linked fullerene (1 nm). These assembled features withstood 3 days of Soxhlet extraction in toluene, as would be expected for covalent binding. Placing the patterned substrates in a solution of a pentathiophene butyric acid chloride and a carboxyl-terminated third-generation benzyl ether dendron also resulted in raised lines corresponding roughly to the height of the newly attached molecule (see the SI). The lines formed by assembly of the dendron onto the amine were stable toward repeated washings with water, but they could be disrupted by immersion in a 1 M NaCl solution or removed entirely with 1 M aqueous acetic acid. Collectively, these results suggest that the electrochemically reduced regions display typical amine chemistry.

Having successfully demonstrated the ability to reductively pattern the benzoquinone-modified surface, we next explored oxidative patterning of the same surface. Initial attempts with existing AFM-based oxidative methods<sup>7a,c</sup> were unsuccessful, as the underlying Si(100) was oxidized instead of the monolayer itself, resulting in SiO<sub>2</sub> patterns that were not amenable to directed assembly. This observation was rationalized by the incomplete passivation of the underlying Si(100) due to the low coverage of the surface with **1**. To better passivate the surface, the initial benzoquinone-modified surface was treated with propyltrichlorosilane (**4**) to “backfill” the exposed Si(100) binding sites. Propyltrichlorosilane has a carbon chain length similar to that of the tether of **1**, so it was expected that a mixed monolayer consisting of **1** and **4** would be sufficiently dense to facilitate constructive oxidative patterning while still rendering the benzoquinone reductively active.

Consistent with propyltrichlorosilane modification, the mixed monolayer **3** was thicker ( $0.75 \pm 0.24$  nm) and had a substantially increased contact angle ( $92 \pm 4^\circ$ ) relative to surface **2**. Evidence for constructive oxidation of the alkane-based monolayer was provided by replication of a common contact-mode-imaging artifact encountered for oxidized organic monolayers<sup>12</sup> as well as by the reactivity of the oxidized patterns to chlorosilanes, which afforded raised lines roughly corresponding to the length of the molecule (see the SI). Together, these results indicate constructive oxidation of the alkane-based monolayer to form oxygen-rich functionalities such as carboxylic acids in preference to oxidation of the underlying silicon to form SiO<sub>2</sub>.

Because the combination of oxidative and reductive patterns on **3** generated two orthogonal functionalities on the same surface, the directed assembly of two different molecules through bifunctional patterning could be attempted, as shown in Figure 3. Therefore, a pentathiophene dimethylchlorosilane, **5**, was assembled on the oxidized patterns while C<sub>60</sub> was assembled onto the reduced patterns. The observed height difference of ~2.5 nm between **5** and C<sub>60</sub> corresponds to the difference in the sizes of the two different objects (see the SI). Directed assembly of both p-type and n-type materials on the same surface highlights the possibility of surface assembly of complementary heterogeneous structures in the construction of more complex nanoarchitectures.

In summary, we have developed a patterning methodology using SPL that enables the patterning in a single lithography session of

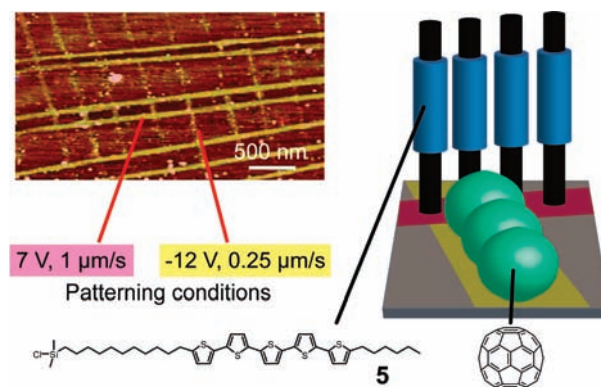


**Figure 3.** Multiplexed directed assembly onto bifunctionally patterned **3**. (left) AFM height image ( $Z$  axis = 10 nm). (right) Graphical representation of the assembled surface, with C<sub>60</sub> deposited on the reductive patterns ( $-12$  V,  $0.25 \mu\text{m/s}$ ) and **5** deposited on the oxidative patterns ( $7$  V,  $1 \mu\text{m/s}$ ). All of the patterns were drawn at 70% relative humidity.

two different functionalities onto the same surface for subsequent use as separate templates in directed assembly. The sub-100 nm feature sizes of both the reductive and oxidative lines are some of the smallest to date for a bifunctional system. Bifunctional patterning strategies may provide a general platform for applications in hybrid top-down/bottom-up fabrication, directed surface-based construction of elegant supramolecular assemblies,<sup>13,14</sup> or production of sensors and devices that may require complementary combinations of organic or inorganic materials.

**Acknowledgment.** Financial support for this research by the National Science Foundation (Award CMMI-0751621) under UC Berkeley’s SINAM is gratefully acknowledged.

**Supporting Information Available:** Detailed syntheses, experimental methods, and additional figures. This material is available free of charge via the Internet at <http://pubs.acs.org>.

## References

- (1) Bratton, D.; Yang, D.; Dai, J.; Ober, C. K. *Polym. Adv. Technol.* **2006**, *17*, 94.
- (2) Mendes, P.; Yeung, C.; Preece, J. *Nanoscale Res. Lett.* **2007**, *2*, 373.
- (3) (a) Taylor, P. G.; Lee, J.; Zakhidov, A. A.; Chatzichristidi, M.; Fong, H. H.; DeFranco, J. A.; Malliaras, G. G.; Ober, C. K. *Adv. Mater.* **2009**, *21*, 2314. (b) Slocik, J. M.; Beckel, E. R.; Jiang, H.; Enlow, J. O.; Zabinski, J. S.; Bunning, T. J.; Naik, R. R. *Adv. Mater.* **2006**, *18*, 2095. (c) Xu, H.; Hong, R.; Lu, T.; Uzun, O.; Rotello, V. M. *J. Am. Chem. Soc.* **2006**, *128*, 3162. (d) Im, S. G.; Bong, K. W.; Kim, B.; Baxamusa, S. H.; Hammond, P. T.; Doyle, P. S.; Gleason, K. K. *J. Am. Chem. Soc.* **2008**, *130*, 14424.
- (4) Paxton, W. F.; Spruell, J. M.; Stoddart, J. F. *J. Am. Chem. Soc.* **2009**, *131*, 6692.
- (5) (a) Backer, S. A.; Suez, I.; Fresco, Z. M.; Rolandi, M.; Fréchet, J. M. *Langmuir* **2007**, *23*, 2297. (b) Fresco, Z. M.; Suez, I.; Backer, S. A.; Fréchet, J. M. *J. Am. Chem. Soc.* **2004**, *126*, 8374.
- (6) Piner, R. D.; Zhu, J.; Xu, F.; Hong, S. H.; Mirkin, C. A. *Science* **1999**, *283*, 661.
- (7) (a) Maoz, R.; Frydman, E.; Cohen, S. R.; Sagiv, J. *Adv. Mater.* **2000**, *12*, 725. (b) Xie, X. N.; Chung, H. J.; Tong, D. M.; Sow, C. H.; Wee, A. T. S. *J. Appl. Phys.* **2007**, *102*, 084313. (c) Yang, M.; Wouters, D.; Giesbers, M.; Schubert, U. S.; Zuilhof, H. *ACS Nano* **2009**, *3*, 2887. (d) Braunschweig, A. B.; Senesi, A. J.; Mirkin, C. A. *J. Am. Chem. Soc.* **2009**, *131*, 922.
- (8) Li, Y.; Maynor, B. W.; Liu, J. *J. Am. Chem. Soc.* **2001**, *123*, 2105.
- (9) (a) Hodneland, C. D.; Mrksich, M. *J. Am. Chem. Soc.* **2000**, *122*, 4235. (b) Rohde, R.; Agnew, H.; Yeo, W.; Bailey, R.; Heath, J. *J. Am. Chem. Soc.* **2006**, *128*, 9518. (c) Wang, B.; Liu, S.; Borchardt, R. T. *J. Org. Chem.* **1995**, *60*, 539.
- (10) Hoepfener, S.; Maoz, R.; Sagiv, J. *Nano Lett.* **2003**, *3*, 761.
- (11) Fresco, Z. M.; Fréchet, J. M. *J. Am. Chem. Soc.* **2005**, *127*, 8302.
- (12) Wouters, D.; Willems, R.; Hoepfener, S.; Flipse, C. F.; Schubert, U. S. *Adv. Funct. Mater.* **2005**, *15*, 938.
- (13) Jonkheijm, P.; Hoeben, F. J. M.; Kleppinger, R.; van Herrikhuyzen, J.; Schenning, A. P. H. J.; Meijer, E. W. *J. Am. Chem. Soc.* **2003**, *125*, 15941.
- (14) Yamamoto, Y.; Zhang, G.; Jin, W.; Fukushima, T.; Ishii, N.; Saeki, A.; Seki, S.; Tagawa, S.; Minari, T.; Tsukagoshi, K.; Aida, T. *Proc. Natl. Acad. Sci. U.S.A.* **2009**, *106*, 21051.

JA101627E